Hindawi
International Journal of Optics
Volume 2022, Article ID 8160054, 16 pages
https://doi.org/10.1155/2022/8160054

Research Article

The Effectual Spectrum Defragmentation Algorithm with Holding Time Sensitivity in Elastic Optical Network (EON)

S. Selva Kumar,[1] J. Kamalakannan,[2] R. Seetha,[2] N. Asha,[2] Kiruba Thangam Raja,[2] S. Sree Dharinya,[2] M. Sucharitha,[3] and S. Kalaivani[2]

[1]*School of Computer Science and Engineering (SCOPE), VIT-AP University, Amaravathi, India*
[2]*School of Information Technology and Engineering (SITE), Vellore Institute of Technology, Vellore, India*
[3]*School of Electronics Engineering (SENSE), VIT-AP University, Amaravathi, India*

Correspondence should be addressed to S. Selva Kumar; selvakumar.s@vitap.ac.in

Received 3 June 2022; Revised 1 September 2022; Accepted 14 October 2022; Published 11 November 2022

Academic Editor: A. Cartaxo

The elastic optical network (EON) fulfills the upcoming generation network requirements such as high-definition videos, high bandwidth demand services, and ultra-high-definition televisions. The key issues in EON are routing spectrum assignment and spectrum fragmentation for spectrum allocation. The spectrum fragmentation issues are resultant in poor consumption of spectrum resources and an increase in the new connection blocking. A flexible defragmentation algorithm must utilize more spectrum resources with a high transmission rate. This paper presents a new multiconstrained defragmentation algorithm (MCDFA) for elastic optical networks. The MCDFA addressed two key issues: spectrum allocation for new connections and then reconfiguring the existing connections in a nondisruptive manner. The first-last-exact fit spectrum allocation policy assigns the spectrum slots during the new connection request. It splits each light path request by disjoint/ nondisjoint and by efficiently handling the small fragmented slots in spectrum resources. The simulation results are evaluated using standard metrics such as bandwidth blocking probability, bandwidth fragmentation ratio, and spectrum utilization gain. The results also demonstrated that our proposed algorithm generates promised solution to EON's routing, spectrum assessment, and fragmentation issues.

1. Introduction

The number of Internet users has increased due to online classes during the pandemic situation, high-definition videos, high-volume cloud data centres, social broadcasting applications, and mobile users' demand for high-capacity data transmission networks. The current scenarios, such as the growth of smartphones, cloud data centres, and next-generation network models (6G), may grow in the upcoming years which will lead to network traffic increase by 25% and creates open research issues for the research. The future generation network must support efficient and high data transmission with an affordable budget. The DWDM (dense wavelength division multiplexing) technology provides a good solution for high-demand bandwidth applications; it is still insufficient due to the fixed spectrum grid nature. The elastic optical network (EON) is the future technology of optical networks that provides capable resolutions for upcoming traffic demands. The EON is a sliceable spectrum grid technology with a 12.5 GHz minimum spectrum interval called frequency slots (FSs) or spectrum slots. The main objective of EON is that flexible FSs provide high-capacity network transmission without wasting unnecessary spectral resources [1].

The networks must achieve the quality of service in any situation and adapt to traffic demands. The OFDM (orthogonal frequency division multiplexing) is the recent modulation format that adopts modern wireless and wired network connection technologies. The OFDM supports high data rate transmission with cost-effectiveness. The EON is the OFDM-based flexible spectrum and high-capacity network. The EON transmits more than 400 Gb/s bandwidth

requests as a single channel over a longer distance. The EON also supports various data rates without wasting spectrum resources because it supports recent flexible transceivers. The key issues recognized in the EON and currently many research articles focused on the routing and spectrum assignment (RSA) problem. The RSA problem involves selecting the route and assigning spectrum sources for every incoming demand. However, recent research algorithms are trying to resolve the spectrum allocation problem with less blocking probability in the dynamic traffic environment. In the EON, all the arrivals are treated as the Poisson distribution, and the holding time of each request (demands in Gbps) is the exponential distribution.

The EON design enforces the RSA problem with three essential constraints: (1) light path continuity constraint, i.e., every incoming arrival must provide spectrum continuity up to reaching the destination, (2) the contiguous allocation of spectrum slots or frequency slots (FSs), that is, spectrum portion must allocate continuously without any in-between breaks of the slot, (3) all light paths must be nonoverlapped; that is, each connection must separate without any interference between other connections. Figure 1 shows the three constraints of the RSA problem in EON architecture with different incoming demands.

The consecutive connection demands arrive for the establishment in real time, but some GHz or less than the demand that tearing down may lead to inaccessible FSs that cause spectrum fragmentation. Spectrum fragmentation refers to the presence of accessible spectrum FSs in the spectrum field that are either not contiguous or not properly aligned, making it difficult to allocate for an incoming connection request. The spectrum fragmentation issue results in a poor utilization spectrum, increased connection blocking, and reduced transmission speed. For these reasons, a good defragmentation algorithm is essential to increase the efficiency of flexible spectrum resources in the EON network.

Figure 2 displays two adjacent links with 10 frequency slots (FSs) divided as the spectrum. In dynamic traffic behavior, the link spectrum displays fragmentation, and only 3 and 4 slots are available for concurrent usage of new light paths. If the new light path request needs two contiguous slots, only FSs 3 and 4 may be allotted. Only 40% of the spectrum is used for both two links, and other portions of the spectrum are wasted due to bandwidth fragmentation.

2. Related Works

Recent literature concepts and methodologies address the difficulty of spectrum fragmentation and defragmentation in EON. The classification of different defragmentation algorithms are briefly discussed in [2, 3]. Spectrum reallocation schemes are proposed in [4] based on a hitless manner. The nondisruption of continuous defragmentation methods is straddling proactive to reactive strategies for each optical light path establishment. Some approaches provide the solution by reconfiguring the service of the light path due to the suppression effect of the fragmentation bandwidth [5–7]. The authors in [6] do not provide any reallocation or skip the spectrum slot called the recurring push-pull approach, which gradually allocates the spectrum slots one by one. The hop returning method allows skipping and reallocation of spectrum slots when establishing the connection if any free space slots could be occupied without any traffic disruption [6]. Ba et al. proposed the fragmentation scheme that permits switching to the primary and backup paths. The light paths can switch the primary or backup paths; both can be rearranged through defragmentation. The success of the switch path approach in [7] and Sawa et al. [8] enhance the approach that enables the backup path to be rerouted in the supposedly 1 + 1 path protected in the EON. Pederzolli et al. [9] proposed a new fragmentation metric. It is helpful to measure spectrum fragmentation during the dynamic traffic demands and provides a good solution in the super channel or different modulation formats. Yang et al. presented a metric to calculate the difference in holding time of each light path and found the exact free spectrum slots for the next state to avoid fragmentation in dynamic traffic demands [10]. In [11], authors proposed a new metric called the fragmentation factor (FF) to select the suitable spectrum slots for each incoming demand at high traffic diversion. Zhao et al. [12] proposed an approach to completely allow shorter holding time light paths and longer holding time light paths to share the remaining shared partitioning slots of the spectrum.

Chatterjee et al. [13] presented a new impairment-conscious spectrum allocation method for the EON to reduce the connection request blockings in the network. No dispersion adjusting device is used in that proposed spectrum allocation approach to suppress the dispersion impact. This approach separates every new request into two categories longer light path and shorter light path based on the threshold selection algorithm. Then, the proposed method used both first fit and last fit spectrum allocation policies based on the required FSs of each request. Next, the aware state algorithm was used to allocate spectrum resources among the partitioned slots, which reduces the number of blockings in the dynamic situation [14]. The two metaheuristic approaches [15] moderate defragmentation complexity and decrease blocking probability in dynamic connection demands, namely, DF-ants and DF-gen algorithms derived from origin ant colony optimization. Zhang et al. [16] provided a clear explanation of defragmentation problems in terms of four subproblems: (1) how to migrate to heavy traffic, (2) how to reconfigure existing connections, (3) when reconfiguration is required, and (4) choosing which light path to reconfigure aids in reducing fragmentation and minimizing the number of light paths reconfigurable in EON. The authors in [17] presented a new proactive and reactive reconfiguration algorithm based on the holding time of each existing connection of the light path. A service-driven fragmentation-aware (SDFA) resource allocation method is proposed in [18]. The SDFA algorithm tries to improve resource efficiency by avoiding fragmentation by considering the existing path and adjacent links. The SDFA approach concentrates on determining fragmentation while taking into account both fragmentation on the utilized path and fragmentation impact on the

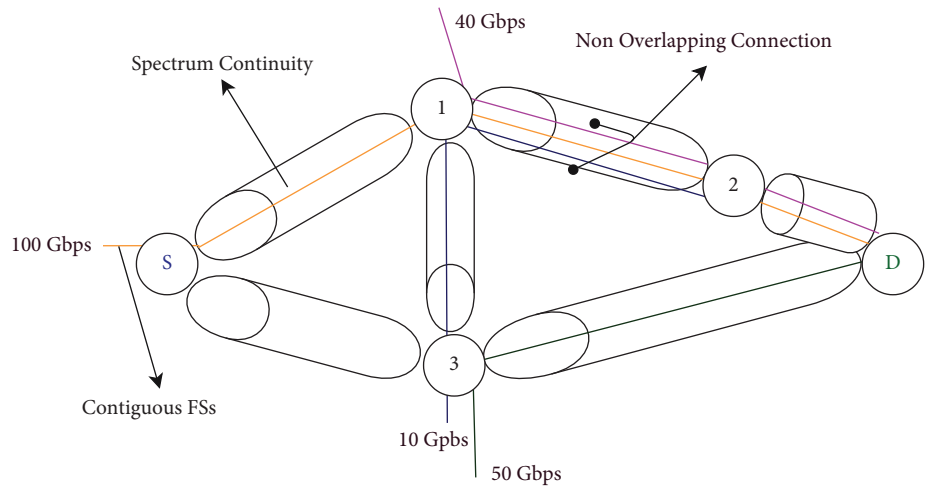

Figure 1: Three constraints in the RSA problem.

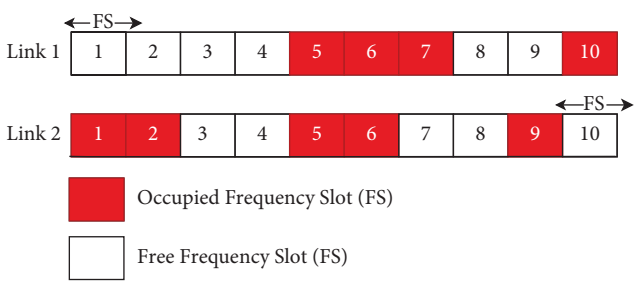

Figure 2: Spectrum fragmentation in the EON.

adjacent links. The fragmentation-aware routing, modulation format, core, and spectrum allocation (RMCSA) approach minimizes future network fragmentation with two proactive heuristic algorithms [19]. The minimum path contiguity is chosen from among the spectral resources proposed in the path contiguity reduction (PCR)-link contiguity reduction (LCR) algorithm and tries to reduce the complexity of path selection and allocation problems [20]. Elastic optical networks' (EONs) features provide the user with a high standard quality experience. For example, quality must depend on all protocol stack layers while receiving high-definition videos on the Internet. The challenge is to design a good algorithm for the RSA problem that satisfies EON constraints and aware fragmentation in slot assignment.

Numerous defragmentation algorithms are discussed in related works. Those works are classified into two categories: (1) proactive approaches and (2) reactive approaches. The proactive approaches are elusive measures of FSs to sidestep fragmentation without waiting for a new connection demand [6–8, 13, 14]. The reactive approaches raise when new demands may be blocked due to defragmentation [9–11, 15, 16]. Both proactive and reactive approaches are categorized as rerouting or without rerouting during the light path establishment. Both approaches are generally important to reduce the number of standing light paths affected by defragmentation and produce the quality of transmission. In addition, the existing defragmentation algorithms use a variety of spectrum allocation policies, such as the first fit, the last fit, random fit, first–the last fit, most used, least used, and first–the last fit, the last fit, random fit, and exact fit. Let us assume when the light path request attains consecutively, establishing the connection one after another even if that is shared as an identical link. But, if more than a single request is started at a similar time, then it does not share an identical link.

In Figure 3, for example, the spectral ch2 released connection holds seven slots of 12.5 GHz (assume Ch2 carries 400 Gbps with 16 QAM mentioned as a green dotted line) and can be empty. If the four slots can be preoccupied with any 100 Gbps signal, it may result in 3 fragmented slots. The fragmentation problem can be resolute by either trying to reduce the fragmentation or performing a more effective defragmentation process to resolve it. When establishing a new connection, the first option is the number of slots that need to accommodate less than the number of unutilized spectrum slots that are possible for spectral expansion. The next option is a good defragmentation process that improves the spectrum consumption by taking effective measures on recognized dynamic traffic. There are two options in the defragmentation process mentioned in Figure 3(a) reroute existing light path with or without reassigning the spectrum. The established light path can be rerouted to an alternate path from the existing routing table that satisfies RSA constraints. This approach, also called nonhitless defragmentation, disrupts the connection due to a change in the route path. The second approach reassigns the spectrum slots keeping the same optical route path. This approach performs unceasingly moved spectrum wavelengths and then following receivers. This approach has no disruption in connection and traffic delay because the optical route path is not changed. This approach is also called hitless defragmentation; it is very effective and provides more spectrum utilization without any traffic disruption.

The flexible network architecture is mandatory to accomplish hitless defragmentation. In [21], authors provide new network architecture. In that architecture, they use universal transceivers instead of flexible transceivers, as

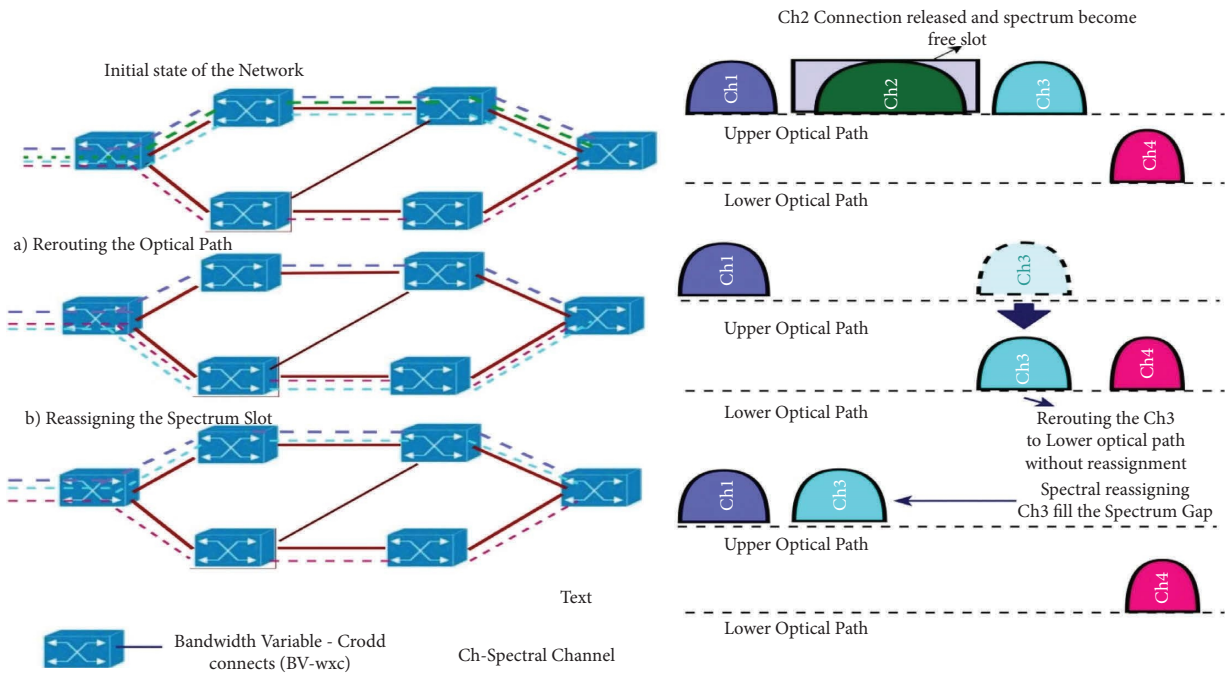

FIGURE 3: Fragmentation options (a) without reassigning the spectral channel and (b) reassigning the spectrum channel fill the spectrum gap when the other connection is released (ex. Ch2).

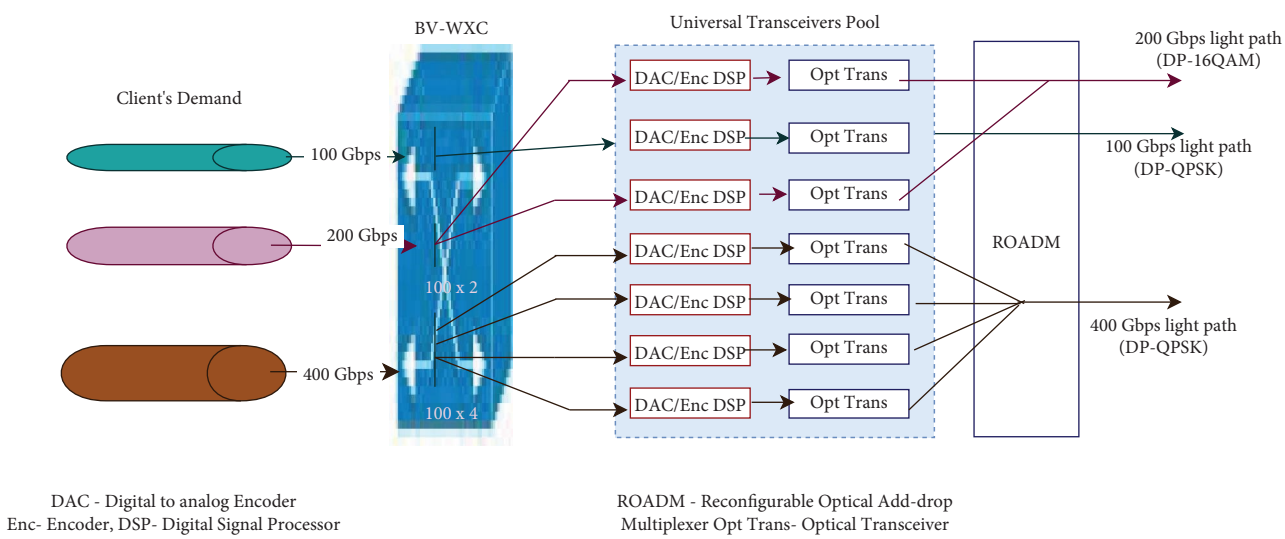

FIGURE 4: Network architecture for hitless defragmentation.

shown in Figure 4. The flexible transceivers may satisfy the client's request, but it is not enough to perform a defragmentation operation because all the devices involved cannot be coordinated with all other devices with the centralized network controller under the dynamic situation. So, the authors design transceivers that are placed in the universal transceiver pool, so there are no transceivers at the client's end.

The hitless defragmentation approach can be achieved using the push-pull or hop-tuning method. In the push-pull method, the properties of the connections are relocated to contiguous spectrum slots along the unchanged original connection route path shown in Figure 4. The get returning of the light path fills the spectrum gap proactively when the existing connection is left from the network and reduces the fragmentation of the spectrum [22]. The push-pull is incomplete if inaccessible and available FSs cannot be touched. The hop tuning method is not necessary if the FSs are adjacent to the existing connection, and it can be moved to any available FSs in the current optical path [23].

The hop tuning approach has an additional feature; it can allow multiple connections simultaneously without the need for an additional transmitter. The main objective of this paper is to reduce the fragmentation complexity consequence by updating and controlling the bandwidth dynamically for every light path, both single and multipath

routing techniques. The next objective is to minimize the reconfiguration rate and increase the network's transmission speed with minimum bandwidth blockings. This work is also considered the holding time of every request and physical layer impairments of the network.

The nondisruptive methods provide minimal service disruption by using existing connections which are relocated from FSs link 0 to link 3 if the in-between spectrum on the same route is unrestricted (i.e., Link 1 and Link 2). So, the reconfiguration has some limits, reducing the connection blocking probability and offering more benefits. The crucial question is whether the existing algorithms utilize more spectrum resources with minimal service disruption.

For example, let us consider that 7 connections are occupied spectrum slots in Figure 5. Figure 5(a) shows the faultlessly well-utilized spectrum resources, but they remain in a shorter duration. The shorter lifetime connections (Con5 and Con3) are torn down from the network, and fragmentation occurs in the spectrum of resources. The better way to reconfigure the connection is by using their lifetime or holding time in the network, which allows for maintaining the nonfragmented condition of the network longer than is possible with factoring holding-time information illustrated in Figure 5(b). This work aims to provide a new defragmentation method with a good reconfiguration technique. The proposed method is combined with both proactive and reactive defragmentation schemes. The proposed reconfiguration schemes try to spectrum provision for incoming new requests organized with other existing connections. The symbols used in the proposed defragmentation algorithm are predefined in Table 1.

3. Multiconstrained Defragmentation Algorithm

This work combined proactive and reactive approaches to defragmentation algorithms with additional constraints to better utilize spectrum resources and avoid traffic disruption. Both proactive and reactive approaches can be restricted to their policies. For example, the connection request that arrives cannot be predicted and difficult to calculate the available spectrum slots for future requests when the proactive approach tries to consolidate the spectrum may not be enough to suit incoming arrivals, so the connection is blocked. In the reactive approach, some connections conflict with a new connection request when reconfiguring the connection request. Our algorithm can consider these limitations and try to balance both approaches. The next consideration of this approach is the crosstalk issue in the EON. When the propagation process is affected severely in the optical signal due to the crosstalk, the identical spectrum slot overlaps with contiguous spectrum cores, and inter-crosstalk occurs. As a result, the optical path carries one or more request demands in the same source, and the destination pair crosses channel interference between the other connections. Even the orthogonal frequency division multiplexing (OFDM) is not entirely orthogonal when sometimes carrying either one or two guard bands necessary to avoid crosstalk and improve the quality of service (QoS). Therefore, calculating the holding time of each connection must be essential to prevent the fragmentation issue in the network. This work utilized a metric used in [10] to calculate the holding time of each connection and provide accurate spectrum allocation of each demand without the fragmentation problem defined in Equation (1). At the instant when the new connection request arrives in the network, the remaining holding time $H_t(l)$ for existing connections in the link is calculated as

$$\mathbf{H_t(l)} = \left(\sum_{i=0}^{\mathbf{F}-1} \frac{\left|\left|\mathbf{t}_i + 1 - \mathbf{t}_i\right|\right|}{\mu}\right) * \left(\frac{\mathbf{CRC_b(l)} - \mathbf{CRC(l)}}{\mathbf{CRC_b(l)}} + 1\right). \tag{1}$$

Let us assume the F of frequency slots in a link, where $H_t(l)$ is the holding time of the link, t_i is the holding time of the ith frequency slots (FSs) in a link, $|t_i + 1 - t_i|$ is the value of the holding time difference between two adjacent already occupied frequency slots in a link, μ is the mean value of the holding time of incoming demands, CRC is contiguous-slot remained capacity, and $CRC_b(l)$ is a link before assigning spectrum for the present request. The metric is helpful to find the minimum holding time difference between FSs in a link and helps in a possible way to assign the spectrum. The calculated exact FSs of each incoming demand are very effective and avoid physical layer impairments such as ASE (amplified spontaneous emission) and XPM (cross-phase modulation). The required FSs for establishing the new connection request are defined in Equation (2) based on the work in [13].

$$\mathbf{FS_s} = \left[\frac{\mathbf{D}}{\mathbf{S_{slot}} \cdot \mathbf{M}}\right] + \mathbf{Gb}, \tag{2}$$

where D is the demand bit rate in Gbps, $\mathbf{S_{slot}}$ is the spectrum granularity usually 12.5 GHz used in OFDM-based network model, M is the respective modulation format based on distance, and Gb is the number of slots needed as guard bands for transmission. For instance, if the 1 bit-per-symbol modulation BPSK is used for every FS or equivalently for every subcarrier FS, then the base capacity may be measured in terms of the required bandwidth. By increasing the modulation level, there is the possibility of multiplying the capabilities of FSs. Furthermore, QPSK offers 2, whereas 8-QAM and 16-QAM provide 3 and 4 base capacities per FS, respectively. For example, a 30 Gbps demand with modulation format QPSK requires 3 FSs ((30/25) + 1) for transmission. The dynamic guard band-based allocation improves the spectrum efficiency but takes more system complexity. The currently available spectrum slots are calculated based on the following equation:

$$\mathbf{T_l} = \sum_{\mathbf{i}=0}^{\mathbf{F}-1} \left|\mathbf{S_{l,i}} - \mathbf{S_{l,i+1}}\right|, \tag{3}$$

where $\mathbf{S_{l,i}}$ is a binary variable considered as 1 when the FS_i is previously used or engaged in the link l of the path P_i, and it is denoted as 0. $\mathbf{T_l}$ is the integer variable representing the total number of available free spectrum slots, P is the candidate optical path, l is a link of the path P_i. If $Tl \geq 1$, then it is treated as free slots and their positions over the link (l) are counted.

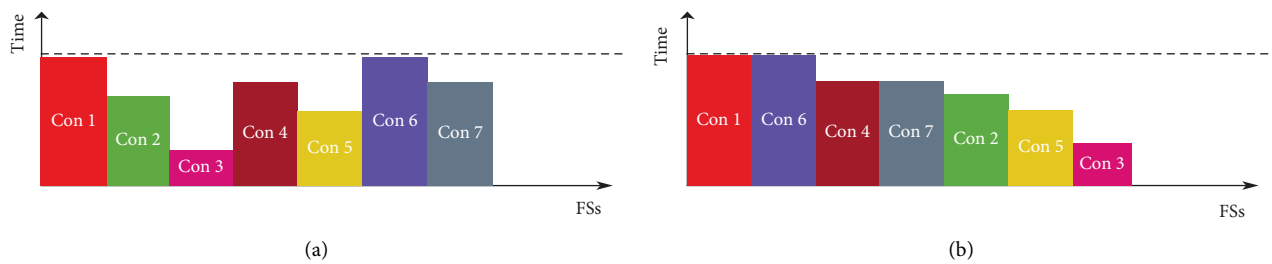

Figure 5: Example scenario spectrum assignment. (a) Normal spectrum allocation without holding time and (b) SA with holding time-based.

Table 1: Symbols used in predefinitions.

Symbol	Description
B	Bandwidth
D	Client demand
$\mathbf{E}_l$ and $\mathbf{E}_p$	The spectrum continuity
FSs	Frequency slots
Gb	Guard band
Ht	Holding time
L	The number of links is present between all nodes.
M	Modulation format
N	Network
P	Candidate path
$\mathbf{P_r}$ and $\mathbf{N_r}$	Current route and next route
R	All routes between the source and the destination
$\mathbf{R_c}$	Connection to be reconfigured
Rt	Routing table
S	Space
s and **d**	Source and destination
$\mathbf{S_{slot}}$	The spectrum granularity in EON
T	Time
$\mathbf{Blk}(\mathbf{FS}_l)$	The size of the present huge block
Ch and $\mathbf{FI}_r$	Optical channel and the minimum number fragmentation index

After calculating all free slots over the link, we find the spectrum continuity from existing free slots as per Equation (4). A disguise $\mathbf{E}_l$ is created when $\mathbf{T}_l \geq 1$, based on the calculated free slots, and their places over the link (**l**) can be defined as the following equation:

$$\mathbf{E_l} = \begin{cases} 1, & FS\text{: Occupied,} \\ 0, & FS\text{: Free slot.} \end{cases} \tag{4}$$

The same way creates one more mask called $\mathbf{E_p}$ for each candidate's path. E_p is used to fix the spectrum arrangement for each candidate optical path contingent on $\mathbf{E_l}$ (including the position of the slot index). So, both $\mathbf{E_l}$ and $\mathbf{E_p}$ are used to identify the spectrum continuity from the existing available slots and nonoverlapping between connections.

The first-last-exact fit spectrum allocation policy used in this algorithm [24] can decrease the number of blockings in the connection demands, and it picks the uppermost indexed slots from the currently available slot list. The first last exact fit policy splits each light path request by disjoint and nondisjoint, efficiently handling the small fragmented slots. The first last exact fit policy splits each light path request by disjoint and nondisjoint, efficiently handling the small fragmented slots. It is depicted in Figure 6.

The first step of the RSA problem is route selection. The route is selected based on the link cost (distance) from k of all possible routes in the network between the source and the destination pair. Once the route is selected, we consider the basic constraints of RSA: spectrum continuity and contiguous constraint before the allocation phase. The following functions can be applied to choose alternative channels of the network path.

$$\mathbf{Ch} = \max_{ch\epsilon_{p,N}} \left\{ \min_{l\epsilon p} \max \left[FS_l(c), E_{l\text{higher}}(c) \right] \right\}, \tag{5}$$

and

$$\mathbf{Ch} = \max_{ch\epsilon_{p,N}} \left\{ \min_{l\epsilon p} \min \left[E_{l\,\text{Lower}}(c), E_{l\,\text{Higher}}(c) \right] \right\}, \tag{6}$$

where $\mathbf{ch}\epsilon_{p,N}$ are the vacant channels on the path p over network N. $E_{l\,\text{Lower}}(c)$ and $E_{l\,\text{Higher}}(c)$ are the current unused FSs in the upper and lower side of the channel path. The value of $FS_l(c)$ is equal to the total number of FSs in the current channel. From Equation (5), we thus allow choosing the channel which is the maximum amount of the unused FSs available in the path, and it will help retain the spectrum allocation quicker as possible. Equation (6) is used to maintain the balancing of the free FSs on both sides of every channel path.

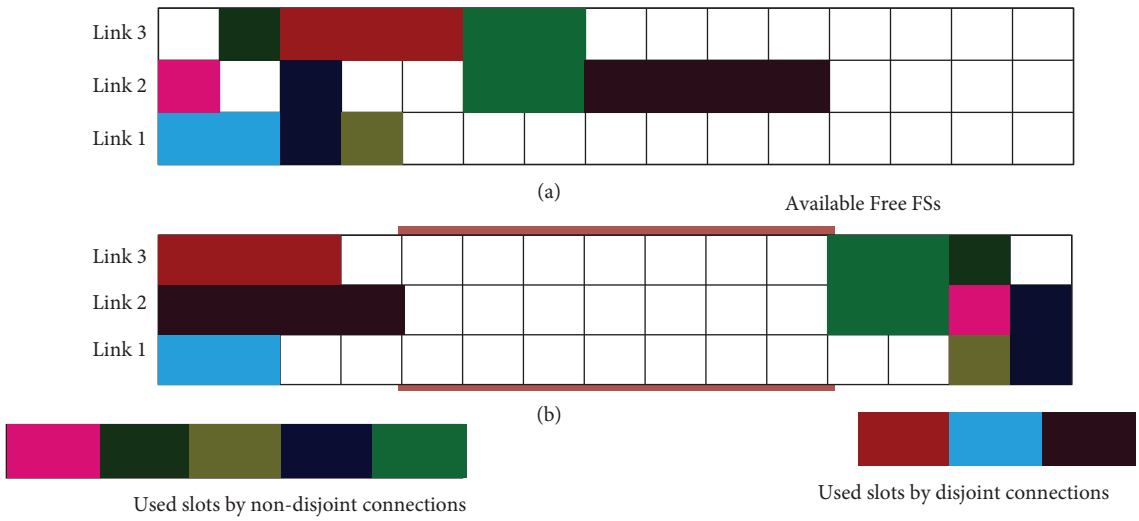

Figure 6: The first-last-exact fit spectrum allocation policy.

The next step is calculating the minimum number fragmentation index (FI_r) available on the route equation as follows:

$$\mathbf{FI_r} = \frac{\textbf{maximum continous FSs avilable on the route}}{\mathbf{T_{lr}}}, \quad (7)$$

where $\mathbf{T_{lr}}$ represents the total number of FSs available on the route. For this technique, the route can prefer the maximum availability of $\mathbf{FI_r}$ for assigning the connection over other available routes**.** The overall network fragmentation index is calculated as per the following equation:

$$FI_{\text{spec-Time}}^{\text{Network}} = \frac{1}{|L|} \sum_{\forall l} FI_{\text{spec-Time}}(l). \quad (8)$$

$FI_{\text{spec-Time}}$ is denoted as spectrum and time fragmentation metric used in [17], |L| represents the number of links presented in the network, and $FI_{\text{spec-Time}}(l)$ is the spectrum time-based fragmentation index in each link. The defragmentation algorithms usually work with two principles mentioned earlier in this chapter: proactive defragmentation and reactive defragmentation. The multi-constrained defragmentation algorithm (MCDFA) is presented in Table2.

The proactive algorithms are used in every cycle when the existing connection leaves the network and the new arrival request is not assigned to the network. It has tried to consolidate each unoccupied FS and realign the spectrum in a contiguous manner. The reactive algorithms are tried to admit the new connection demand only by reconfiguring existing connection resources without clashing new arrivals. The reactive algorithms deal with a new connection request, whether it can accommodate the network or reject it.

The MCDFA combines proactive and reactive defragmentation algorithms with additional constraints to avoid the number of blocks. The first two steps of the MCDFA algorithm initialize the physical network parameters such as the number of nodes present in the network, the number of links between each node, the distance between the nodes, and the current network traffic load. The new connection request arrives at the network, then the algorithm reacts and gathers the information about the source, destination, size of the request (in Gbps), and holding time of the request in step 3. Then, the next step of the algorithm finds all possible routes between the requested source and the destination. After discovering all routes between the source and the destination, the next stage is to construct the routing table along with fixing the modulation format based on the route selection, i.e., initially creating the routing table with each route having a different modulation format, and the number of FSs needed for the connection establishment also vary for every route. After constructing the routing table in the next stage, each route is tested for connection establishment (step 4).

In algorithm step 5, we calculate the number of unoccupied FSs presented in each network channel. After selecting the route and appropriate modulation technique, the needed frequency slots for the requested connection are computed. The core selection is based on the dynamic core selection procedure [18]. We choose the core with the highest predetermined priority out of the group of cores that have been categorized and ranked for the same bandwidth as the connection that is currently in use. If no core is selected, we choose the core that has the lowest priority according to the classification for each of the other bandwidths. Once enough contiguous FSs are available in the current route, it satisfies the RSA constraints. Then, the demand allocated to connection establishment otherwise finds possibilities to assign in the upper link and lower link of the channel with the same constraints and allocation policy (step 5.), Step 6 reconfigures periodically to all current routes when some connections may leave the network. The third stage of the algorithm finds the rerouting possibility from the existing connection of the current route to the new route without any disruption in the network. This algorithm reconfigured the existing connection using the hitless method [2]. When the connection request cannot be assigned due to crossing the fragmentation threshold in a link, the defragmentation algorithm reacts and reconfigures the network. Figure 7 illustrates the sample scenario of reconfiguring existing connections in the route. In

Table 2: Multi-constrained defragmentation algorithm (MCDFA).

Multi-constrained defragmentation algorithm (MCDFA)
Step 1: initialize the network status
Step 2: initialize the network parameter **N(V, L)**
V is the *number of nodes,* and *L* is the *number of links between the nodes*
Step 3: each arrivals **R(s,d,D,Gb)**
s-*Source*, d-*Destination*, D-*Demand*, and Gb-Gurd bands
Step 4: find all possible routes($\mathbf{k}_i$)
Construct routing table **Rt** with respective modulation format and number of FSs using Equation (2)
Step 5: **for each** $\mathbf{k}_i$**do**
Find the best RSA constraint (N, D) for $\mathbf{n}_{\mathbf{FSs}}^{\mathbf{min}}$ from Equation (5) for spectrum allocation
if the exact route is found from Equation (7) **then**
Choose the channel from Equation (6) for
RSA ← route + spectrum allocation policy
Allocate $\mathbf{R}_i$ to the network
else
Reallocate neighboring connections of N,
Find the best RSA constraint (N, D) for $\mathbf{n}_{\mathbf{FSs}}^{\mathbf{min}}$ from Equation (5) for spectrum allocation
if an exact route from Equation (7) is found **then**
Choose the channel from Equation (6) for
RSA ← route + spectrum allocation policy
Allocate $\mathbf{R}_i$ to the network
else
if FSs cannot assign && $FI_{spec-Time}^{Network} > FI_t$**then**
goto step 6:
else
Block the connection request $\mathbf{R}_i$
end if
end if
Step 6: $\mathbf{R_c}$**:** *set of connections that may be a necessity for reconfiguration*
$\mathbf{R_l}$**:** *connection leaving*
$\mathbf{P_r(x)}$**:** *present route*, $\mathbf{N_r(x)}$**:** *next route*
if $\mathbf{R_c}$*Reconfigure* **Then**
for each link $\mathbf{R_c} \in \mathbf{P_r(x)}$ **then**
$\mathbf{R_c}$ ← Connection path share with some link $\mathbf{R_l}$ (which is occupied high **FSs**)
While $\mathbf{R_c} \neq \emptyset$ **do**
$\mathbf{R_i}$ occupied the lowest **FSs** in $\mathbf{R_c}$
if $\mathbf{R_i(Ht(l))}$*shifted upper to lower optical path* **then**
$\mathbf{R_c}$ shares **FSs** with $\mathbf{R_i}$ (*which is Occupied High* **FSs**)
end if
$\mathbf{R_c} \leftarrow \mathbf{R_c} \backslash \{\mathbf{R_i(Ht(l))}\}$
end while
end for
else
for each link $\mathbf{R_i} \in \mathbf{P_r(x)}$ **and** $\mathbf{R_c} \in \mathbf{P_r(x)}$ **then**
if new available **FSs** ≥ minimum required **FSs** for $(\mathbf{N_r(x)})$ **then**
Reassign route $\mathbf{P_r(x)}$ **to** $\mathbf{N_r(x)}$
end if
end for
end if
Step 7: restart network parameters
Step 8: **end loop**

that figure, a new connection request con6 comes to the network waiting for spectrum assignment, but the current situation is that the connection cannot accommodate due to nonaligned FSs. However, reconfigure Con2 and Con3 so that FSs are available for connection Con6 and that connections are relocated to other FSs without overlapping. Generally, the network transmission got affected or disrupted in rerouting, but our algorithm rerouting process made only the connection establishment done before the new request arrival. So, the rerouting process does not affect the current path in the network. The first-last-exact fit allocation policy is to avoid small adjoining accessible slots, which may be troublesome to use for upcoming light path demands.

4. Experimental Results

The proposed algorithm is evaluated through the simulations on three different topologies, (1) The National Science Foundation Network (NSFNET) 14 nodes, 21 bidirectional optical links [25], and (3) 11 nodes and 26 links high-capacity COST239 ultraoptical network [26]. The main performance metric is the bandwidth blocking probability (BBP) or blocking probability of connection request that is used to check the efficiency of the defragmentation procedure of the proposed algorithm. The BBP was calculated as per the following equation:

$$\mathbf{BBP} = \frac{\sum \mathbf{Q_R}}{\sum \mathbf{Q_B}}, \tag{9}$$

where $\sum \mathbf{Q_R}$ represents the total number of arrival requests, and $\sum \mathbf{Q_B}$ represents the total number of requests that are blocked. The bandwidth fragmentation ratio (BFR) represents the amount of inaccessible, noncontiguous slots and nonaligned spectrum portions in the network among the adjoining, assigned, and connected FSs. The BFR displays the existing fragmentation condition of the network at any particular point in time. Usually, when the BFR increases, the chance of bandwidth blocking probability also increases. The proposed MCDFA algorithm efficiently handles and manages the BFR by reconfiguring the light path and defragmentation of the FSs in the links that do not interrupt the overall QoS of the spectrum. Equation (10) calculates the network's BFR values of specified links [21].

$$\Upsilon_l = \begin{cases} 1 - \dfrac{\text{enorm}\mathbf{Blk}(\mathbf{FS_l})}{\mathbf{N} - \sum(\mathbf{FS_l})}, & \text{if } \sum(\mathbf{FS_l}) < \mathbf{N}, \\ 0, & \text{if } \sum(\mathbf{FS_l}) = \mathbf{N}, \end{cases} \tag{10}$$

where enorm$\mathbf{Blk}(\mathbf{FS_l})$ is the size of the present huge block in l, N is the number of the FSs each link, and $\sum(\mathbf{FS_l})$ specifies the amount assigned FSs in link l. The BFR formula for the complete network indicated as $\mathbf{BF_{Rnet}}$ is in the equation,

$$\mathbf{BF_{Rnet}} = \frac{\sum_{\forall l \varepsilon \mathbf{L}} \tau \Upsilon_l}{|\mathbf{L}|}. \tag{11}$$

In the equation mentioned previously, L specifies the group of links and $|L|$ denotes the number of links in the entire network. The next performance metric is the spectrum utilization gain (SUG), which shows how many network resources are utilized effectively without unnecessarily

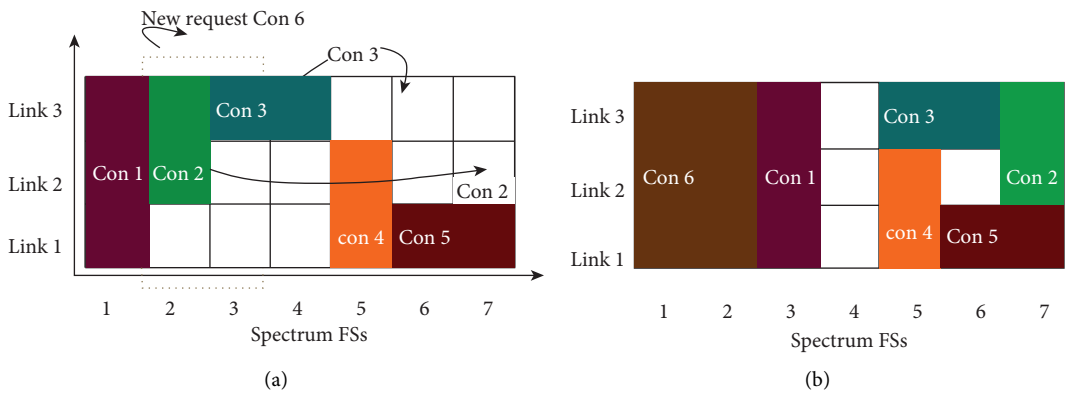

Figure 7: The network reconfiguration (a) before the reconfiguration (b) con 6 accommodated after possibly reconfiguring con2 and c3.

refusing the number of connections due to poor FS distribution created by fragmentation [21]. The defragmentation technique is very important to achieve more spectrum utilization because it robustly manages the reconfiguration and disturbance rate without negotiating the overall throughput of the network. Spectrum utilization (SU) is subject to space, time factors, and bandwidth mentioned in Equation (12). Spectrum utilization is defined by how it is spaced out geographically, how it shares frequencies or uses orthogonal frequencies, and how it shares the time division.

$$\mathbf{SU} = \mathbf{S} * \mathbf{T} * \mathbf{B}. \tag{12}$$

The spectrum utilization gain is calculated as per the equation,

$$\mathbf{SUG} = \frac{\mathbf{G}}{\mathbf{SU}}, \tag{13}$$

where G is the gain achieved after defragmenting slots. The quality metrics are examined under various network traffic volumes during testing. The Shannon entropy fragmentation measure is calculated on either the unused or utilized spectrum [27]. Entropy measures the level of defragmentation in a link as per the equation,

$$\mathbf{DF_l} = \frac{\sum \mathbf{CFs_l}}{\mathbf{m}}, \tag{14}$$

where $\mathbf{CFs_l}$ are the number of position changes of the FSs in link l, and m is the total number of FSs per link. The overall network defragmentation of the network is measured by the equation,

$$\mathbf{DF_{net}} = \frac{\sum \mathbf{DF_l}}{|\mathbf{L}|}. \tag{15}$$

The effects of defragmentation are determined by the temporal characteristics of the specified network load. The intercrosstalk (IC-XT) has a massive impact on multicore fibers' (MCFs) transmission. Avoid overlapping spectrum slots with the same serial number across neighbouring cores of an optical fiber link while allocating FS and cores to various transmission requests. The threshold is set at −30 dB. Whenever the crosstalk value exceeds −30 dB, the transmission becomes easier to block. The performance of MCDFA is evaluated by Monte Carlo simulation with modulation format parameters (BPSK, QPSK, 8QAM, 16-QAM, 32-QAM, and 64-QAM) as per Table 3 [28, 29]. The MATLAB 2018a is used for the simulation, and the network parameters for the simulations are presented in Table 4. The connection demands are generated by an arbitrary method with a Poisson arrival rate λ. The service time of each arrival $\Delta\mathbf{st}$ with unit mean time μ was used in order to calculate network load Erlangs as $\lambda * \mu$ [30, 31].

Under two scenarios, the experimental simulations are performed with the standard metrics of bandwidth blocking probability, bandwidth fragmentation ratio, spectrum utilization gain, holding time analysis, and the network reconfiguration rate. In the first scenario, the algorithm is tested in low traffic load up to 100 Erlang and then high traffic load up to 900 Erlang with each arrival request treated as 0.2% as a short holding time and 0.9% long holding time. As a result, the frequency slot is equally distributed between 2 and 16 slots. In the next scenario, the bandwidth of connections is tested dynamically, and the requested FSs are uniformly distributed between 2 and 12 FSs.

The results are compared with existing well-performed algorithms Df-Gen [15], PRDF [17], FACP-RMCSA [19], and Min PCR-LCR [20]. Every time connections are assigned to the network, it halts some time, then exits from the network and releases used spectral resources. These simulations estimate the influence of the connection holding time on defragmentation. The blocking probability is considered for two of the scenarios which are mentioned in this earlier section. In the first scenario, between 4 and 8 FSs are fixed for short holding time connection requests with traffic load ($\lambda = 1$ to 9) Erlang. The proposed algorithm outperformed well compared to other spectrum allocation policy algorithms. It reduces the number of blockings or rejects the least number of connection requests. Figure 8 shows BP(%) results for short holding time arrivals for both topologies (NSFNET and COST239).

Initially, all algorithms work well up to 200 Erlang. When the traffic load increases after 200 Erlang, some algorithms are insufficient to produce connection assignments for every request. Meanwhile, the Min PCR-LCR and MCDFA algorithms perform well under a small-time arrival scenario. Similarly, the long holding arrivals with uniformly distributed bandwidth are tested as the same traffic load, and

Table 3: The modulation format parameters are used in simulations.

Modulation format	Slot capacity (Gb/s)	Distance to reach (Km)	Bits/symbol
BPSK	12.5	4000	1
QPSK	25	2000	2
8QAM	37.5	1000	3
16-QAM	50	500	4
32-QAM	62.5	250	5
64-QAM	75	125	6

Table 4: The network parameters used in simulations.

Total bandwidth	4400 GHz
The number of frequency slots per link	352 FSs
Frequency slot bandwidth	12.5 GHz
Central frequency	193.4 THz
Data transmission rates	50, 100, 400 Gbps
Input optical signal-to-noise ratio (OSNR)	30 dB
Noise figure	3 dB
Spectrum assignment policy	First-last-exact fit

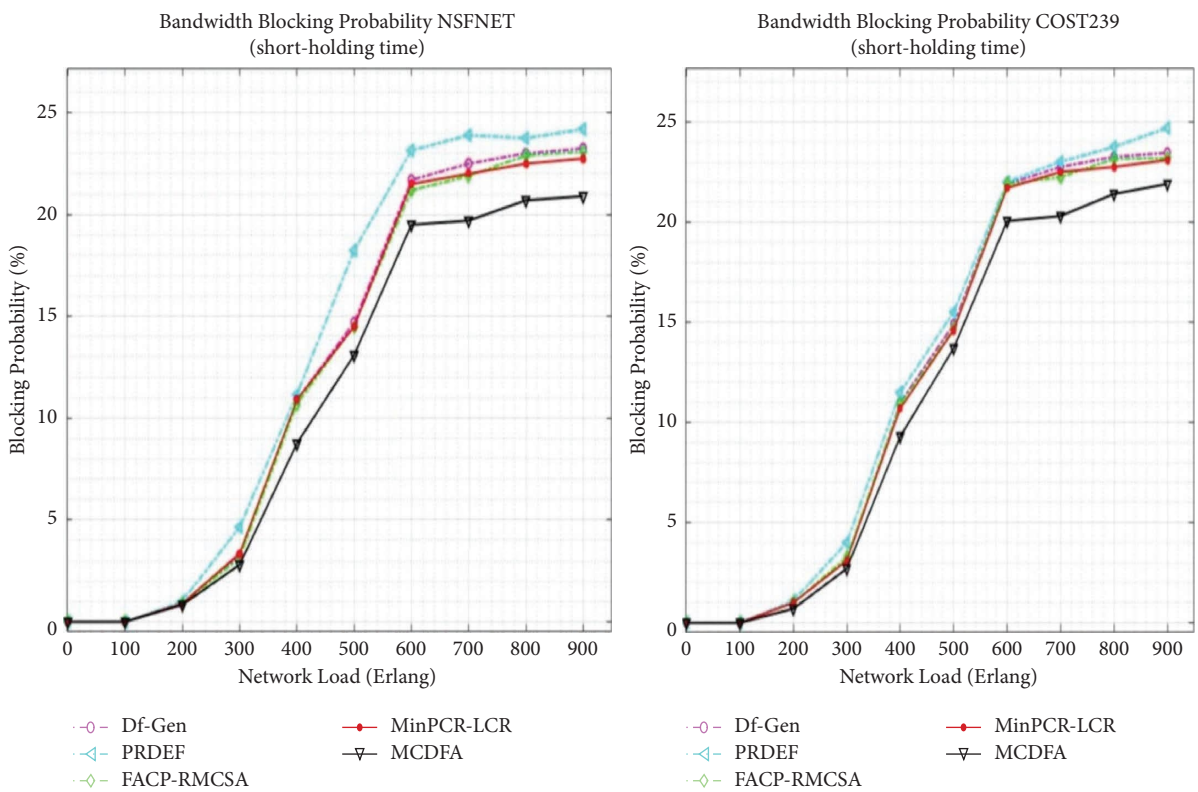

Figure 8: The blocking probability % for NSFET and COST239 under small holding time arrivals (0.2%).

BP (%) results for NSFNET are presented in Figure 9. Both in short holding time and long holding time connection situations, the performance of the MCDFA in terms of BP (%) achieved better results than other algorithms. Because of the high traffic load situation, the proactive algorithms are complicated to reconfigure all the network connections due to resource availability.

In a long holding time arrival situation, when the traffic load around 100 to 200 Erlang Df-gen and PRDEF performed well, but when traffic loads are increased from 300, the MCDFA thrived progressively up to 900 Erlang. The MCDFA produces good results since it retunes the active light path to any unoccupied spectrum FSs. So, the reactive approach retunes the network and rearranges the spectrum slots for upcoming connection demands.

The first-last-exact fit spectrum allocation policy best accommodates the new connection request because it combines both the first-exact fit and the last-exact fit spectrum allocation policies. The first-exact fit policy selects the small amount of indexed FSs from accessible contiguous

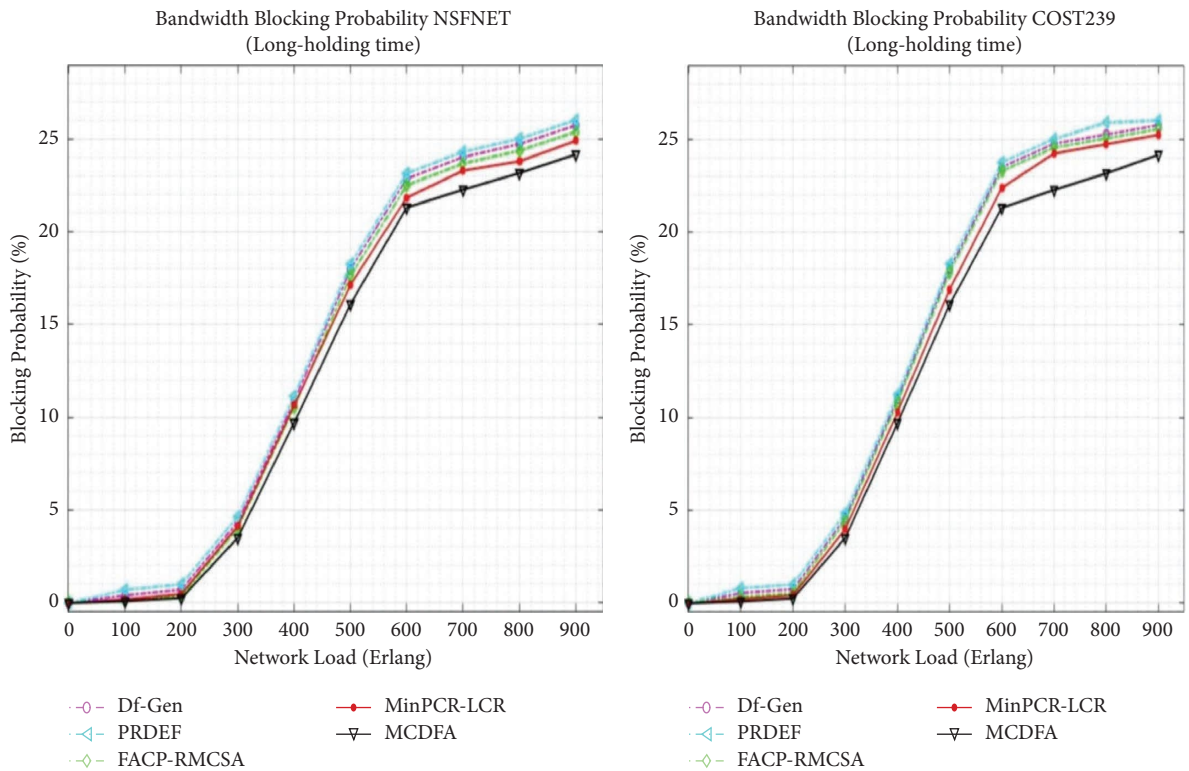

Figure 9: The blocking probability % for NSFET and COST239 under long holding time arrivals (0.9%).

slots, precisely the same amount of FSs needed for connection establishment. So, it is reflected in the results that the MCDFA accommodates more connection requests than recent fragmentation algorithms.

The bandwidth fragmentation ratio (BFR) of MCDFA algorithms for NSFNET and Cost 239 is depicted in Figure 10. When the BP is lesser and fragmentation is also small, the metric BP is not an absolute measure of fragmentation because the rejection rate may change due to the holding time and lack of resources. Nevertheless, the MCDFA proves that it produces the best BFR results compared to other recent algorithms in all cases. The bandwidth fragmentation ratio (BFR) is measured only by how much fragmentation on each link distinctly, but it does not prevent the continuity and contiguous FSs in the link. Here, we need to note one point that sometimes small BFR reproduces those slots that may not be appropriately aligned and itproduces high BP. But the proposed algorithm BFR reflects very low, and the slots are appropriately aligned for clear evidence of that BP rate.

The BFR results are compared with the holding time scenario. In that case, smallholding time arrivals of all algorithm's fragmented ratios are good, but the long holding time scenario of all other algorithms does not produce properly aligned slots for upcoming connections. The MCDFA proved that the BFR is very low even though the traffic load has increased.

Figure 11 shows the entropy results of NSFNET and cost 239 topologies. In general, reactive algorithms do not achieve sufficient entropy values compared with proactive algorithms because the proactive algorithms consolidate the entire FSs and reconfigure the existing connection before admitting the new connection. In both networks, responsive algorithms achieve low entropy than Min PCR-LCR and MCDFA. This situation occurs because other algorithms consider every link's entropy indecently but do not expect the misaligned slots between consecutive links. The MCDFA algorithm addressed spectrum contiguity and wavelength continuity to achieve better entropy than other algorithms.

Figure 12 shows the overall spectrum utilization gain results of NSFNET and Cost 239 topology. The SU value in percentage in the regular network load with first-last-exact fit and after defragmentation is applied. The traffic load gets increased, and the essential spectrum slots also increase. The MCDFA utilized the spectrum resources more efficiently in both networks in a different holding time situation. The MCDFA allocates spectrum by giving priority to routes with the least amount of fragmentation. Also, the routes are allocated with maximum continuous and sequential spectrum slots and a spectrum allocation policy that produces a low level of spectrum fragmentation in any traffic situation. These results achieve better spectrum utilization in all traffic scenarios.

The reconfiguration of connections improves the spectrum utilization for both conditions in the defragmentation algorithm, and it increases with the load values. However, the MCDFA algorithm is the more helpful method, and the spectrum utilization gain is more than 10% at a higher load value of 900 Erlang, as it takes comparatively more incoming connections.

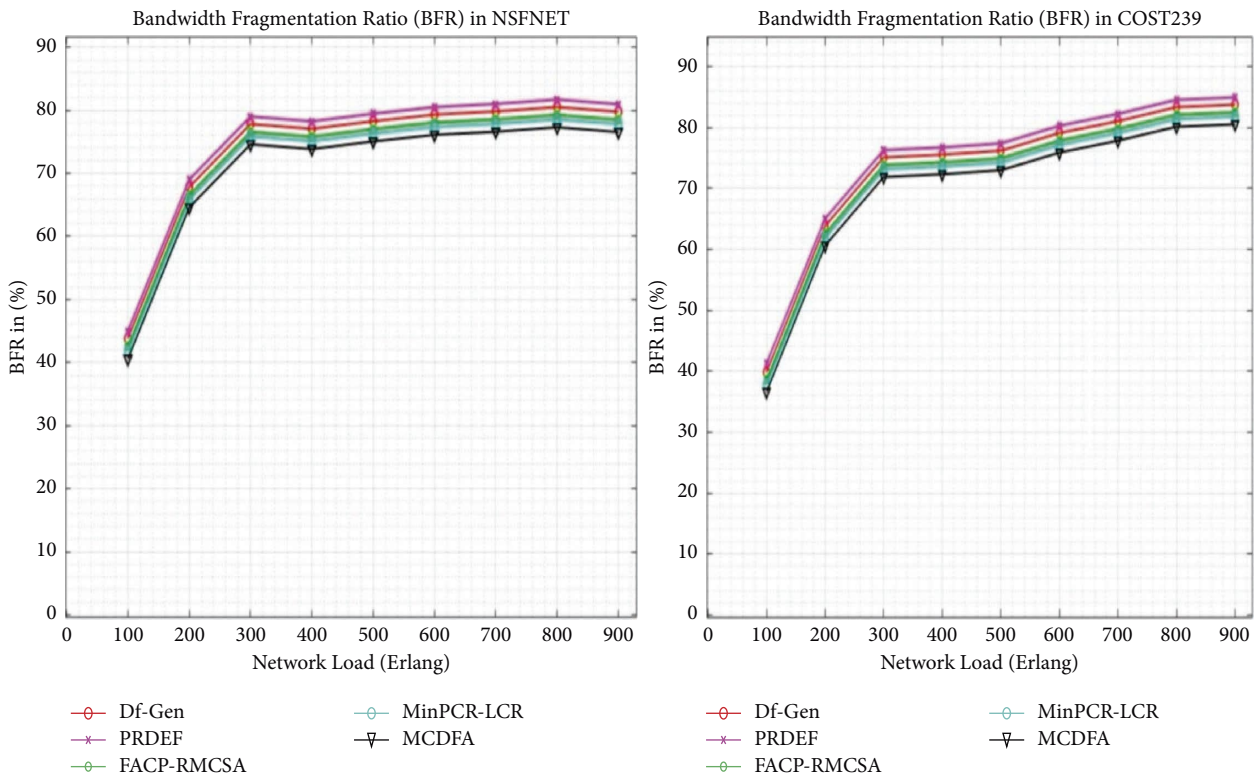

Figure 10: The bandwidth fragmentation ratio (BFR) for NSFET and COST239.

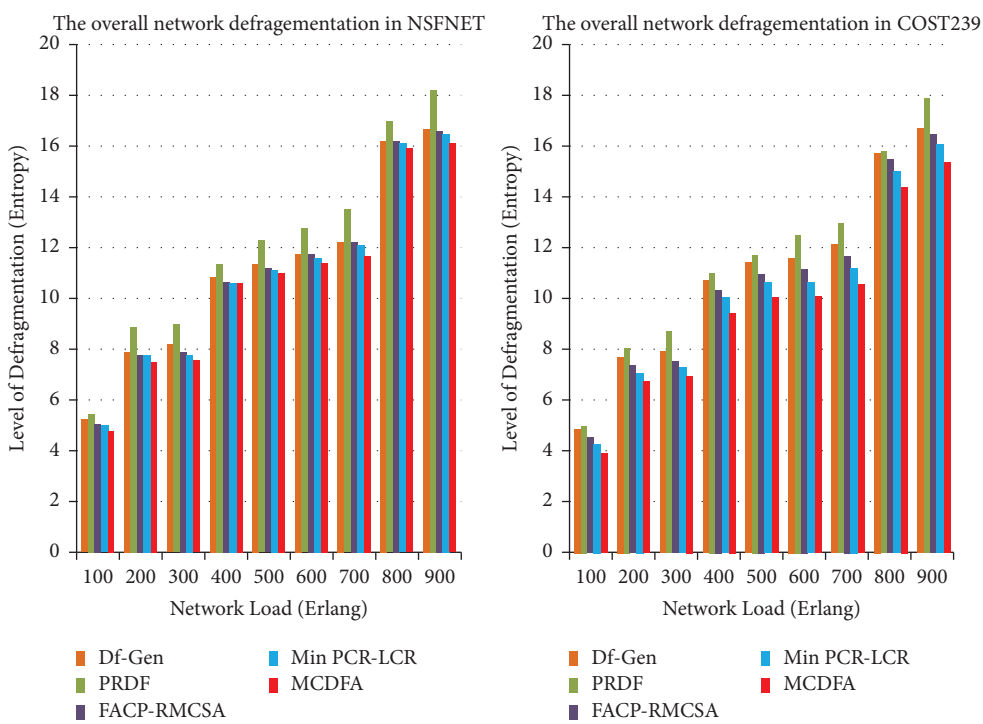

Figure 11: The overall network defragmentation (entropy) for NSFET and COST239.

Figure 13 shows the average number of reconfigured connections in each performed defragmentation in NSFNET and Cost 239. The reconfiguration rate defined as the number of incoming requests is reconfiguring per request. This rate is not identical to the number of successful reconfigures across the all-request set. Since certain connections might cross over the spectrum of another connection, the average number of reconfigurations in the MCDFA algorithm is more significant.

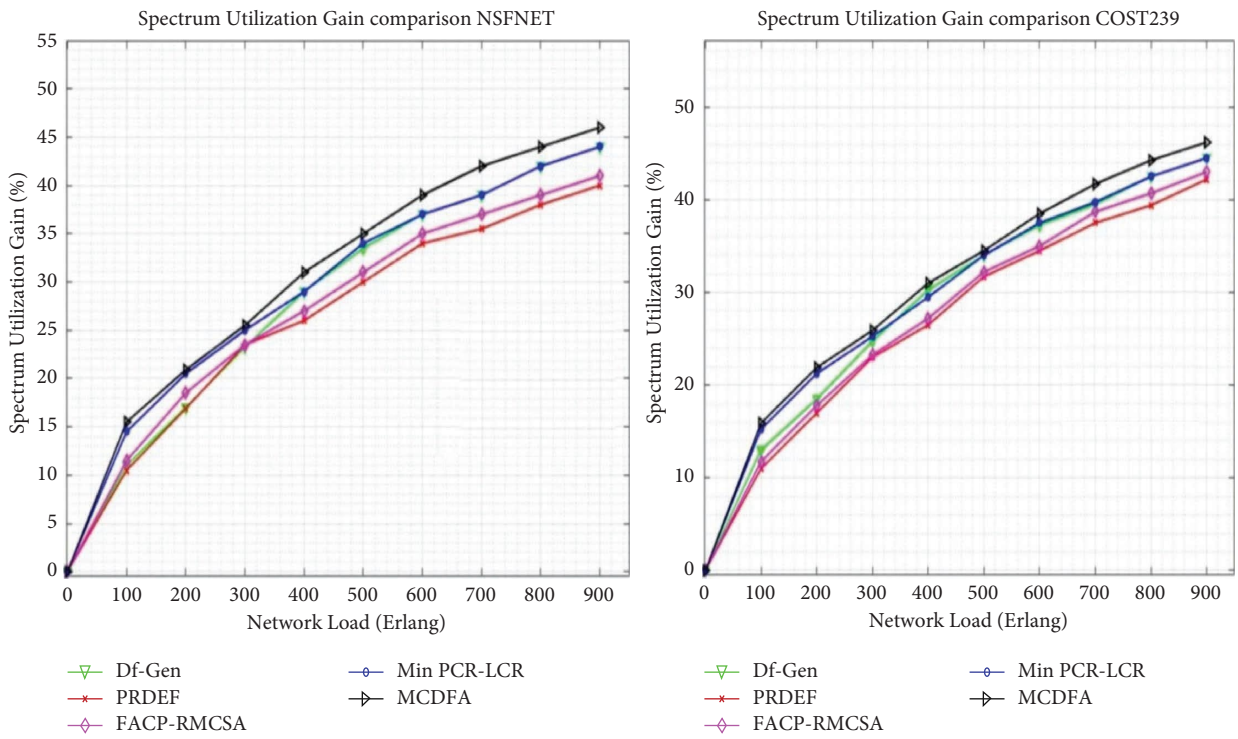

Figure 12: The spectrum utilization gain (SUG) for NSFET and COST239.

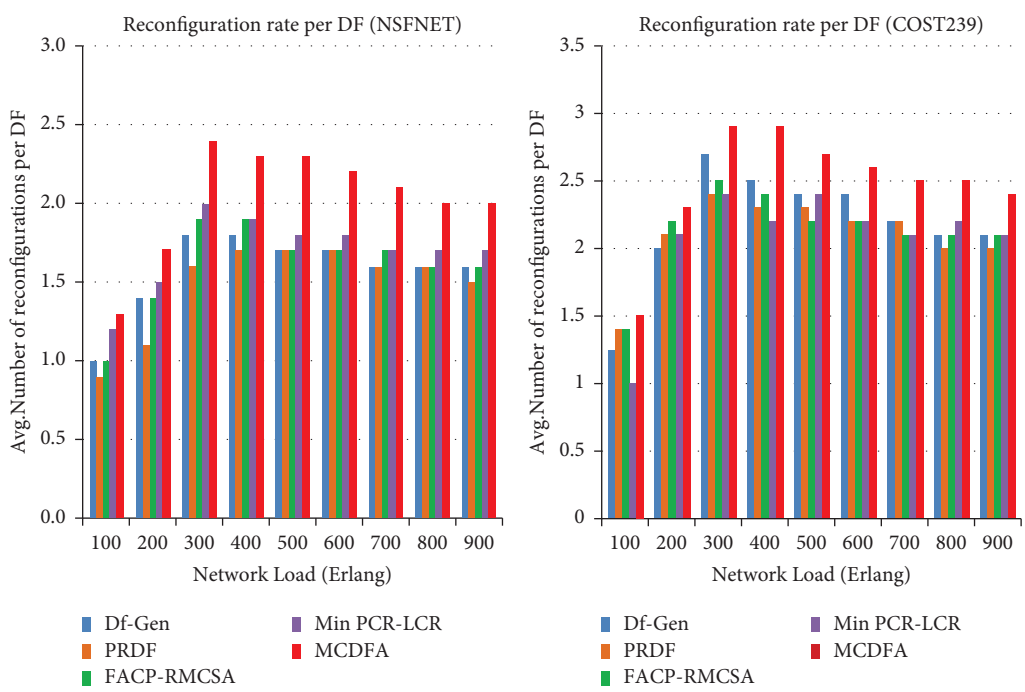

Figure 13: The average number of reconfigured connections performed DF in (NSFNET) and COST239.

However, a higher number of reconfigurations resulted in fewer connection blockings. Usually, the network reconfigures only at the beginning or end of the spectrum allocation process when enough spectral resources are available. After that, reconfigurations grow up to a moderate load (300 Erlang) and drop again at larger loads, as the spectrum is occupied more intensively at higher loads. According to the MCDFA algorithm, a link can be reconfigured only when a new connection node arrives between the source and the destination. Thus, the proactive technique does not interrupt existing communications when reconfiguring a network.

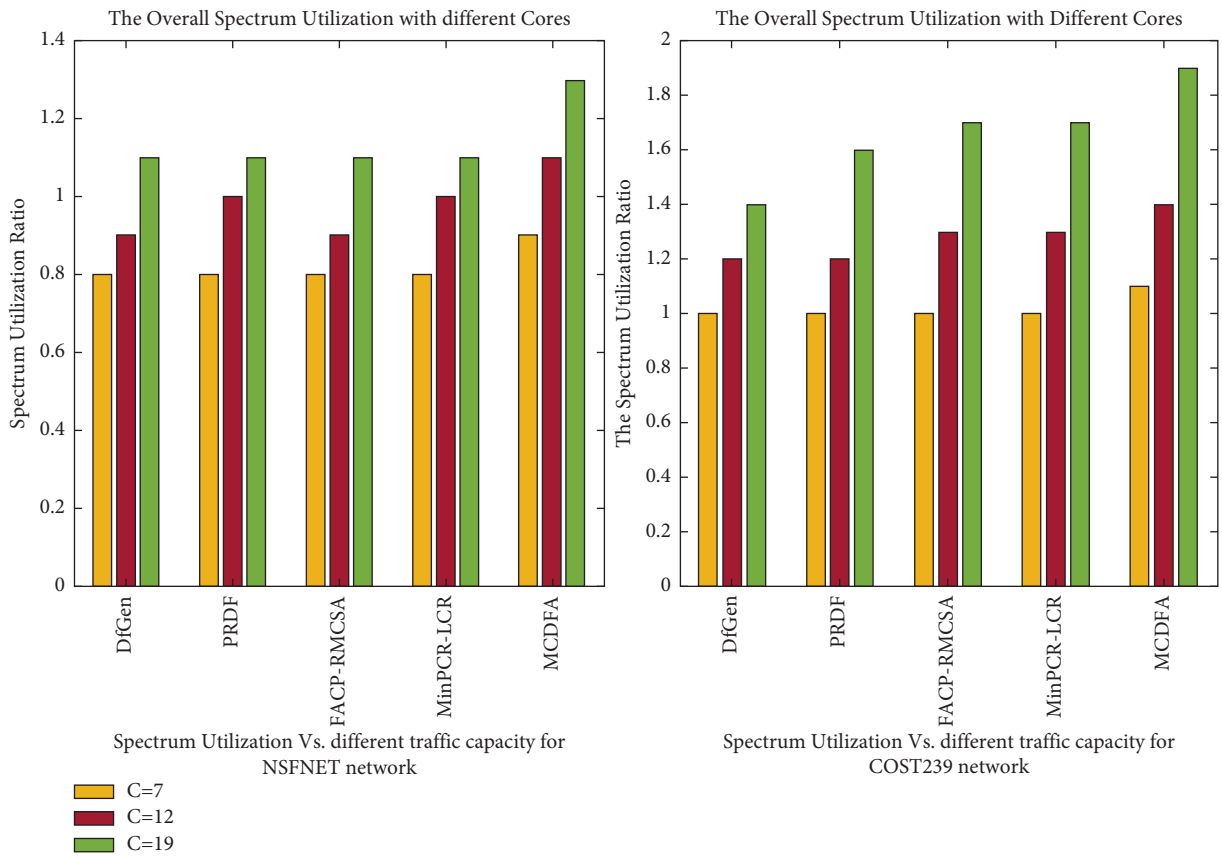

Figure 14: Spectrum utilization vs. different traffic capacities for both network topologies.

Figure 14 depicts overall spectrum utilization proposed algorithm with different cores and existing algorithms that considered both NSFNET and COST239 topologies. This metric is evaluated with varying numbers of core $c = 7$, $c = 12$, and $c = 19$. The cores are important factors to affect the overall spectrum utilization. The number of cores in the network involves overall spectrum utilization. But our algorithm receives the best results compared with other existing algorithms. The Cost 239 topology finds a high 20% overall spectrum utilization compared with the NSFNET topology. However, the connection establishment is concerned with spectrum resource models, bandwidth, goal functions, and dynamic behavior. These operations must be completed quickly for the system to operate in heavy traffic situations.

Furthermore, when the traffic load gets varied, the reconfiguration rate also increases. Therefore, the reconfiguration of the network is necessary according to the traffic variations while setting sideways spectral resources for leased connection light paths and accepting increased traffic demand on the optical network. Therefore, the overall reconfiguration rate of the MCDFA is greater than the other algorithms.

5. Conclusion

This work proposed a new defragmentation algorithm MCDFA that combines proactive and reactive methods with additional constraints such as holding time and spectrum allocation policy. This work proposed a novel nondisruptive reconfiguration scheme that allows much improvement in the connection establishment. A new MCDFA of provisioning is proposed and demonstrated to significantly improve provisioning efficiency utilizing proactive and reactive defragmentation. Specifically, when the network is provided a light load, it improves by 99.8% (low holding time). Furthermore, we find that increased spectrum efficiency does not always indicate increased defragmentation. The overall performance of the MCDFA algorithms produces much better results than other algorithms; it evaluates as per metrics in the literature on the subject against various traffic conditions and the first-last-exact fit spectrum allocation policy. Furthermore, the results are shown that MCDFA uses more spectrum resources than recent algorithms reliably with different holding times on dynamic traffic conditions.

Data Availability

The data used to support the findings of this study are available from the corresponding author upon request.

Conflicts of Interest

The authors declare that they have no conflicts of interest.

References

[1] M. Jinno, H. Takara, B. Kozicki, Y. Tsukishima, Y. Sone, and S. Matsuoka, "Spectrum-efficient and scalable elastic optical path network: architecture, benefits, and enabling

technologies," *IEEE Communications Magazine*, vol. 47, no. 11, pp. 66–73, 2009.

[2] B. C. Chatterjee, S. Ba, and E. Oki, "Fragmentation problems and management approaches in elastic optical networks: a survey," *IEEE Communications Surveys & Tutorials*, vol. 20, no. 1, pp. 183–210, 2018.

[3] S. Fernández-Martínez, B. Barán, and D. P. Pinto-Roa, "Spectrum defragmentation algorithms in elastic optical networks," *Optical Switching and Networking*, vol. 34, pp. 10–22, 2019.

[4] R. Wang and B. Mukherjee, "Provisioning in elastic optical networks with non-disruptive defragmentation," *Journal of Lightwave Technology*, vol. 31, no. 15, pp. 2491–2500, 2013.

[5] S. Ba, B. C. Chatterjee, S. Okamoto, N. Yamanaka, A. Fumagalli, and E. Oki, "Route partitioning scheme for elastic optical networks with hitless defragmentation," *Journal of Optical Communications and Networking*, vol. 8, no. 6, p. 356, 2016.

[6] R. Proietti, C. Qin, B. Guan et al., "Rapid and complete hitless defragmentation method using a coherent RX LO with fast wavelength tracking in elastic optical networks," *Optics Express*, vol. 20, no. 24, Article ID 26958, 2012.

[7] S. Ba, B. C. Chatterjee, and E. Oki, "Defragmentation scheme based on exchanging primary and backup paths in 1 + 1 path protected elastic optical networks," *IEEE/ACM Transactions on Networking*, vol. 25, no. 3, pp. 1717–1731, 2017.

[8] T. Sawa, F. He, T. Sato, B. C. Chatterjee, and E. Oki, "Defragmentation using reroutable backup paths in toggled 1 + 1 path protected elastic optical networks," in *Proceedings of the 24th Asia-Pacific Conference on Communications (APCC)*, Ningbo, China, November 2018.

[9] F. Pederzolli, D. Siracusa, A. Zanardi, G. Galimberti, D. La Fauci, and G. Martinelli, "Path-based fragmentation metric and RSA algorithms for elastic optical networks," *Journal of Optical Communications and Networking*, vol. 11, no. 3, p. 15, 2019.

[10] F. Yang, L. Wang, L. Wang, X. Chen, and Y. Zhao, "Holding-time-aware spectrum allocation algorithm for elastic optical networks," *Optical Fiber Technology*, vol. 41, pp. 155–162, 2018.

[11] R. Dutta, S. S. Krishna, R. Gowrishankar et al., "Fragmentation-aware routing, wavelength and spectrum assignment (RWSA) scheme in flex-grid optical networks," in *Proceedings of the 2017 IEEE International Conference on Advanced Networks and Telecommunications Systems (ANTS)*, Bhubaneswar, India, December 2017.

[12] J. Zhao, B. Bao, H. Yang, E. Oki, and B. C. Chatterjee, "Holding-time- and impairment-aware shared spectrum allocation in mixed-line-rate elastic optical networks," *Journal of Optical Communications and Networking*, vol. 11, no. 6, p. 322, 2019.

[13] B. C. Chatterjee, N. Stol, and E. Oki, "Impairment-aware spectrum allocation in elastic optical networks: a dispersion-sensitive approach," *Optical Fiber Technology*, vol. 61, Article ID 102431, 2021.

[14] J. Wu, S. Subramaniam, and H. Hasegawa, "Efficient dynamic routing and spectrum assignment for multi-fiber elastic optical networks," *Journal of Optical Communications and Networking*, vol. 11, no. 5, p. 190, 2019.

[15] E. J. Davalos, M. F. Romero, S. M. Galeano, D. A. Baez, A. Leiva, and B. Baran, "Spectrum defragmentation in elastic optical networks: two approaches with metaheuristics," *IEEE Access*, vol. 7, pp. 119835–119843, 2019.

[16] M. Zhang, C. You, H. Jiang, and Z. Zhu, "Dynamic and adaptive bandwidth defragmentation in spectrum-sliced elastic optical networks with time-varying traffic," *Journal of Lightwave Technology*, vol. 32, no. 5, pp. 1014–1023, 2014.

[17] S. K. Singh and A. Jukan, "Efficient spectrum defragmentation with holding-time awareness in elastic optical networks," *Journal of Optical Communications and Networking*, vol. 9, no. 3, p. B78, 2017.

[18] S. Fujii, Y. Hirota, H. Tode, and K. Murakami, "On-demand spectrum and core allocation for reducing crosstalk in multicore fibers in elastic optical networks," *Journal of Optical Communications and Networking*, vol. 6, no. 12, p. 1059, 2014.

[19] S. Trindade and N. L. S. da Fonseca, "Proactive fragmentation-aware routing, modulation format, core, and spectrum allocation in EON-SDM," in *Proceedings of the ICC 2019-2019 IEEE International Conference on Communications (ICC)*, Shanghai, China, May 2019.

[20] J. Yuan, D. Zhang, Q. Zhang, X. Li, and Z. Ren, "A routing and spectrum assignment algorithm in elastic optical network based on minimizing contiguity reduction," *Photonic Network Communications*, vol. 38, no. 1, pp. 51–61, 2019.

[21] Y. Aoki, X. Wang, P. Palacharla et al., "Dynamic and flexible photonic node architecture with shared universal transceivers supporting hitless defragmentation," in *Proceedings of the European Conference and Exhibition on Optical Communication*, Amsterdam, Netherlands, September 2012.

[22] F. Cugini, F. Paolucci, G. Meloni et al., "Push-pull defragmentation without traffic disruption in flexible grid optical networks," *Journal of Lightwave Technology*, vol. 31, no. 1, pp. 125–133, 2013.

[23] M. Zhang, Y. Yin, R. Proietti, Z. Zhu, and S. J. B. Yoo, "Spectrum defragmentation algorithms for elastic optical networks using hitless spectrum retuning techniques," in *Proceedings of the Optical Fiber Communication Conference/National Fiber Optic Engineers Conference*, Anaheim, CA, USA, March 2013.

[24] B. C. Chatterjee, N. Kitsuwan, and E. Oki, "Performance evaluation of first-last-exact fit spectrum allocation policy for elastic optical networks," in *Proceedings of the 2017 19th International Conference on Transparent Optical Networks (ICTON)*, Girona, Spain, July 2017.

[25] X. Zhou, W. Lu, L. Gong, and Z. Zhu, "Dynamic RMSA in elastic optical networks with an adaptive genetic algorithm," in *Proceedings of the 2012 IEEE Global Communications Conference (GLOBECOM)*, Anaheim, CA, USA, December 2012.

[26] M. C. Sinclair, "Minimum cost topology optimization of the cost 239 European optical network," *Artificial Neural Nets and Genetic Algorithms*, pp. 26–29, 1995.

[27] Y. Tan, R. Gu, J. Cui, and D. Wang, "Distance-adaptive fragmentation-avoiding spectrum resource allocation for unicast service in flexible optical networks," *Optical Engineering*, vol. 57, no. 8, p. 1, 2018.

[28] I. M. Queiroz and K. D. R. Assis, "A MILP-based algorithm for energy saving in spectrum-sliced elastic optical networks," in *Proceedings of the 2017 9th Computer Science and Electronic Engineering (CEEC)*, September 2017.

[29] S. Selvakumar and S. S. Manivannan, "A spectrum defragmentation algorithm using jellyfish optimization technique in

elastic optical network (EON)," *Wireless Personal Communications*, 2021.

[30] W. Lu, X. Zhou, L. Gong, M. Zhang, and Z. Zhu, "Dynamic multi-path service provisioning under differential delay constraint in elastic optical networks," *IEEE Communications Letters*, vol. 17, no. 1, pp. 158–161, 2013.

[31] S. Selvakumar and S. S. Manivannan, "A spectrum defragmentation algorithm using jellyfish optimization technique in elastic optical network (EON)," 2021, https://www.readcube.com/authentication?client=webapp&redirect=https%3A%2F%2Fapp.readcube.com%2F%3Faction%3Dadd_item%26doi%3D10.21203%2Frs.3.rs-207934%2Fv1.